
Research Article: New Research | Disorders of the Nervous System

Non-cell autonomous regulation of retrograde motoneuronal axonal transport in an SBMA mouse model

Muscle AR regulation of axonal transport in SBMA

Katherine Halievski¹, Michael Q. Kemp¹, S. Marc Breedlove¹, Kyle E. Miller^{1,2} and Cynthia L. Jordan^{1,3}

¹Neuroscience Program, Michigan State University, 108 Giltner Hall, East Lansing, MI 48824-1115.

²Department of Integrative Biology, Michigan State University, East Lansing, MI 48824-1115

³Department of Physiology, Michigan State University, 108 Giltner Hall, East Lansing, MI 48824-1115.

DOI: 10.1523/ENEURO.0062-16.2016

Received: 15 March 2016

Revised: 23 June 2016

Accepted: 14 July 2016

Published: 26 July 2016

Funding: National Institute of Health
NS045195

Funding: Ruth L. Kirchstein National Research Service Award
1F32AR055848-01

Funding: Ruth L. Kirchstein National Institutional Research Service Award
T32-MH070343

Funding: NIH
1R01MH094607-01A1

Funding: NSF
IOS_0951019

Correspondence should be addressed to Cynthia L Jordan, Neuroscience Program and Physiology Department, 108 Giltner Hall, Michigan State University, East Lansing, MI 48824, E-mail: jordancy@msu.edu

Cite as: eNeuro 2016; 10.1523/ENEURO.0062-16.2016

Alerts: Sign up at eneuro.org/alerts to receive customized email alerts when the fully formatted version of this article is published.

Accepted manuscripts are peer-reviewed but have not been through the copyediting, formatting, or proofreading process.

This is an open-access article distributed under the terms of the Creative Commons Attribution 4.0 International (<http://creativecommons.org/licenses/by/4.0>), which permits unrestricted use, distribution and reproduction in any medium provided that the original work is properly attributed.

- 1 **1. Manuscript title:** Non-cell autonomous regulation of retrograde motoneuronal axonal
2 transport in an SBMA mouse model
3
- 4 **2. Abbreviated title:** Muscle AR regulation of axonal transport in SBMA
5
- 6 **3. List of authors and affiliations:**
7 Katherine Halievski¹, Michael Q. Kemp¹, S. Marc Breedlove¹ and Kyle E. Miller^{1,3}, Cynthia L.
8 Jordan^{1,2*}
9
- 10 ¹Neuroscience Program and ²Physiology Department, 108 Giltner Hall, Michigan State
11 University, East Lansing, MI 48824-1115.
12
- 13 ³Department of Integrative Biology, Michigan State University, East Lansing,
14 MI 48824-1115
15
- 16 **4. Author contributions:**
17 MQK, SMB, KEM, and CLJ Designed research; MQK, SMB, KEM, and CLJ Performed
18 research; SMB, KEM, and CLJ Contributed unpublished reagents/analytic tools; KH, MQK,
19 SMB, KEM, and CLJ Analyzed data; KH, MQK, SMB, KEM, and CLJ Wrote the paper.
20
- 21 **5. *Correspondence should be addressed to:**
22 Cynthia L Jordan
23 Neuroscience Program and Physiology Department
24 108 Giltner Hall
25 Michigan State University
26 East Lansing, MI 48824
27 Phone: 517-355-1722
28 FAX: 517-432-2744
29 jordancy@msu.edu
30
- 31 **6. Number of figures:** 4
32
- 33 **7. Number of tables:** 1
34
- 35 **8. Number of multimedia:** 0
36
- 37 **9. Number of words for abstract:** 247
38
- 39 **10. Number of words for introduction:** 708
40
- 41 **11. Number of words for discussion:** 2597
- 42 **12. Funding sources:** This research was supported National Institute of Health grant NS045195
43 (to C.L.J.), a Ruth L. Kirchstein National Research Service Award 1F32AR055848-01
44 (M.Q.K.), a Ruth L. Kirchstein National Institutional Research Service Award T32-MH070343
45 (M.Q.K.), NIH 1R01MH094607-01A1 (K.E.M.) and NSF IOS_0951019 (K.E.M.).
- 46 **13. Conflicts of interest:** The authors declare no competing financial interests.
47

48

Abstract

49

50 Defects in axonal transport are seen in motoneuronal diseases but how that impairment comes

51 about is not well understood. In spinal bulbar muscular atrophy (SBMA), a disorder linked to a

52 CAG/polyglutamine repeat expansion in the androgen receptor (AR) gene, the disease-causing

53 AR disrupts axonal transport by acting in both a cell autonomous fashion in the motoneurons

54 themselves, and in a non-cell autonomous fashion in muscle. The non-cell autonomous

55 mechanism is suggested by data from a unique “myogenic” transgenic (TG) mouse model in

56 which an AR transgene expressed exclusively in skeletal muscle fibers triggers an androgen-

57 dependent SBMA phenotype, including defects in retrograde transport. However, motoneurons

58 in this TG model retain the endogenous *AR* gene, leaving open the possibility that impairments

59 in transport in this model also depend on AR in the motoneurons themselves. To test whether

60 non-cell autonomous mechanisms *alone* can perturb retrograde transport, we generated male61 TG mice in which the endogenous AR allele has the *testicular feminization mutation (Tfm)*, and62 consequently is nonfunctional. Males carrying the *Tfm* allele alone show no deficits in motor63 function or axonal transport, with or without testosterone treatment. However when *Tfm* males64 also carrying the myogenic transgene (*Tfm*/TG) are treated with testosterone, they develop

65 impaired motor function and defects in retrograde transport, having fewer retrogradely-labeled

66 motoneurons, and showing deficits in endosomal flux based on time-lapse video microscopy in

67 living axons. These findings demonstrate that non-cell autonomous disease mechanisms

68 originating in muscle are sufficient to induce defects in retrograde transport in motoneurons.

69

70

Significance Statement

71 Our findings suggest that therapies targeting skeletal muscle could potentially rescue
72 motoneurons from axonal transport dysfunction in neuromuscular disease. Axonal transport is
73 critical for proper motoneuronal functioning and is often impaired in neurodegenerative disease,
74 including spinal bulbar muscular atrophy (SBMA), an androgen-dependent neuromuscular
75 disease linked to a polyglutamine expansion in the androgen receptor (AR). In this study, we
76 show that AR activated by androgens exclusively in skeletal muscle is sufficient to trigger
77 defects in retrograde transport in the motoneurons. Specifically, diseased mice show impaired
78 retrograde labeling of motoneurons *in vivo* and defective endosomal transport in living axons *ex*
79 *vivo*. Thus, one trait of diseased motoneurons, impaired axonal transport, can be conferred by
80 disease processes originating in muscle.

81

82

83

Introduction

84 Projection neurons are particularly susceptible to defects in axonal transport due to their
85 long processes (De Vos et al., 2008; Morfini et al., 2009). This has led to an interest in the role
86 of axonal transport in neurodegenerative diseases in which projection neurons are affected,
87 including motoneurons in spinal bulbar muscular atrophy (SBMA), a progressive neuromuscular
88 disease linked to a CAG expansion mutation in the *androgen receptor (AR)* gene (La Spada et
89 al., 1991). SBMA occurs only in men and is androgen-dependent (Banahmad, 2015; Katsuno et
90 al., 2012). With only one exception (Malik et al., 2011), studies of axonal transport in both SBMA
91 models and SBMA patients suggest this key neuronal process is perturbed and may be an early
92 event in disease (Katsuno et al., 2006; Kemp et al., 2011; Morfini et al., 2006; Piccioni et al.,
93 2002; Szebenyi et al., 2003). How AR disrupts axonal transport, however, is not clear. Evidence
94 suggests that the disease-causing AR can act directly in the motoneuron in a cell autonomous
95 fashion to disrupt axonal transport (Szebenyi et al., 2003) and/or indirectly in a non-cell
96 autonomous manner via the target musculature (Kemp et al., 2011). Understanding where and
97 how AR impairs axonal transport and whether perturbed transport contributes to motor
98 dysfunction in SBMA is critical for developing effective treatments for this disease.

99 That *non-cell* autonomous mechanisms can instigate motoneuronal dysfunction in
100 neuromuscular disease has been the subject of several recent reviews (Ilieva et al., 2009;
101 Jordan & Lieberman, 2008; Sambataro & Pennuto, 2012). Because motoneurons depend on
102 their targets to survive in development (Hamburger & Levi-Montalcini, 1949) and to function
103 normally in adulthood (Navarro et al., 2007), it stands to reason that disease-related dysfunction
104 originating in muscle could trigger dysfunction in the motoneurons. However, whether axonal
105 transport is susceptible to such non-cell autonomous influences has not been firmly established.
106 In these terms, because both motoneurons and muscle function is impaired in disease models
107 of SBMA, they provide an excellent model system for testing whether defects in axonal transport
108 can arise non-cell autonomously.

109 Reports indicate that retrograde transport is impaired in an androgen-dependent fashion,
110 paralleling the loss of motor function, in a myogenic model of SBMA (Kemp et al., 2011). This
111 unique myogenic mouse model expresses transgenic (TG) wild-type (WT) AR only in skeletal
112 muscle at high levels. While these data imply that signals originating in muscle can impair
113 retrograde axonal transport in motoneurons, because AR is also expressed throughout the body
114 in TG animals by virtue of the endogenous *AR* gene, it leaves open the possibility that the effect
115 of androgen on motoneuronal retrograde transport may have also depended on AR acting in
116 other cell types, including the motoneurons themselves. To eliminate this possibility, we
117 generated mice in which the only source of functional AR was from the transgene expressed
118 only in muscle. We did this by passing the transgene into males carrying an endogenous allele
119 for AR that is dysfunctional, the *testicular feminization mutation (Tfm)*, providing a null
120 background for functional AR. Genetic males carrying the *Tfm* allele are insensitive to
121 androgens, exhibiting a female phenotype but have normal motor function (Johansen et al.,
122 2011; Zuloaga et al., 2008). Thus, male mice carrying both the *Tfm* allele of the endogenous *AR*
123 gene, and the AR transgene with its expression controlled by the muscle-specific human
124 skeletal α actin promoter (*Tfm/TG*), have functional AR only in a single cell type—skeletal
125 muscle fibers. This strategy allowed us to ask whether a disease-causing AR allele expressed
126 solely in muscle fibers is sufficient to impair axonal transport in motoneurons via a non-cell
127 autonomous mechanism.

128 Using cholera toxin (CT) to label retrogradely transporting endosomes, we found fewer
129 *labeled* motoneurons in the lumbar spinal cord of motor-impaired *Tfm/TG* males than in the
130 lumbar spinal cord of *Tfm*-only control males with intact motor function, a deficit in *Tfm/TG*
131 males that is comparable to prior results in myogenic TG males on a background of WT AR
132 (Kemp et al., 2011). Analysis of retrogradely trafficking endosomes in living axons of diseased
133 *Tfm/TG* male mice also revealed the same deficit in endosomal flux as found previously (Kemp

134 et al., 2011). The present data confirm that non-cell autonomous mechanisms originating in
135 target muscle fibers of motoneurons can perturb retrograde axonal transport in the motoneurons
136 innervating them.

137

Materials and Methods***Tfm/TG mouse model.***

139 Tfm/TG mice that express functional AR only in skeletal muscle fibers were generated
140 by *in vitro* fertilization. Sperm was harvested for *in vitro* fertilization from a TG male that
141 overexpresses WT-AR specifically in muscle cells (Monks et al., 2007). Female *Tfm* carriers on
142 a C57Bl/J6 background were superovulated and eggs harvested. The *Tfm* allele renders AR
143 protein nonfunctional and causes androgen-insensitivity uniformly throughout the body (He et
144 al., 1991). After fertilization, embryos were transferred into pseudopregnant recipient B6D2F1/J
145 mice. Four founding females were produced that carried both the transgene and the *Tfm* allele.
146 Female offspring carrying both the *Tfm* gene and AR transgene were mated to WT C57Bl/6
147 males to produce the experimental Tfm/TG males.

148 Many Tfm/TG males die at birth, as do TG males with a WT-AR background (Monks et
149 al., 2007). This perinatal lethality is caused by prenatal exposure to endogenous testicular
150 androgens. To enhance perinatal survival of such Tfm/TG males, pregnant dams were treated
151 with the AR antagonist, flutamide. Pregnant Tfm/TG carrier females were injected
152 subcutaneously with 5 mg flutamide in propylene glycol at the nape of the neck from gestational
153 days 15 – 20 (day of mating designated as day 0). Control males used in this study were
154 littermate males that carried only the *Tfm* allele (*Tfm* males) and thus, were exposed to the
155 same prenatal flutamide treatment as Tfm/TG males. Because *Tfm* male mice develop a deficit
156 in androgen production postnatally (Goldstein & Wilson, 1972; Murphy & O'Shaughnessy,
157 1991), Tfm/TG males have low, female-like levels of circulating androgens as adults,
158 comparable to *Tfm* males (Johansen et al., 2011). This means that postnatally Tfm/TG males
159 are asymptomatic (like TG females) and express disease symptoms only when treated with
160 exogenous testosterone (T) to increase T levels to that of normal males (Johansen et al., 2009).
161 All animal procedures were performed in accordance with the [Author University] animal care
162 committee's regulations.

163 ***Adult hormone treatment to induce disease symptoms.***

164 To induce disease symptoms in adult Tfm/TG males, 150 day old Tfm/TG and Tfm male
165 littermates under isoflurane anesthesia received subcutaneous implants at the nape of the neck
166 just below the interscapular fat pad of Silastic capsules containing crystalline T (1.57 mm inner
167 diameter and 3.18 mm outer diameter, effective release length of 6 mm). Such T implants result
168 in serum T levels comparable to that of adult gonadally intact males (Johansen et al., 2009).
169 After five days of treatment, the efficiency of retrograde transport was assessed in two different
170 ways (as detailed below): retrograde labeling of motoneuronal cell bodies with horse radish
171 peroxidase (HRP) injected into muscle, and active transport of fluorescently-labeled endosomes
172 in living axons of the sciatic nerve. In each case, the label was conjugated to cholera toxin (CT).
173 Forelimb grip strength was monitored using a grip strength meter (Columbus Instruments) in
174 Tfm/TG males and their Tfm male brothers during androgen treatment, beginning just prior to
175 implanting T capsules (day 0), and then on days 1, 2, 3, 4, and 5 of treatment. Means and
176 standard errors are calculated and N = number of animals/group are reported in the figure
177 captions.

178

179 ***Retrograde labeling of spinal motoneurons***

180 Spinal motoneurons were retrogradely labeled by injecting CT B conjugated to horse radish
181 peroxidase (CT-HRP; 1 μ l of 0.2% CT-HRP/muscle; List Biological Labs, USA) into the anterior
182 tibialis (AT) muscles of isoflurane anesthetized mice. Once mice recovered from anesthesia,
183 they were returned to their home cage. After 12 hrs to allow CT-HRP to retrogradely transport to
184 motoneuronal cell bodies, mice were re-anesthetized with an intraperitoneal injection of sodium
185 pentobarbital. Once deeply anesthetized, mice were perfused with 0.9% saline followed by cold
186 0.1 M phosphate buffer (pH 7.4) containing 0.8% paraformaldehyde and 1.25% glutaraldehyde.
187 Spinal cords were dissected out and placed in the same fixative for 5 h at 4°C, after which they

188 were transferred to a 10% phosphate-buffered sucrose solution and held overnight at 4°C. The
189 following day, spinal cords were transversely sectioned on a freezing, sliding microtome at 40
190 µm. Sections were reacted with tetramethylbenzidine (TMB) for histological visualization of HRP
191 (Park et al., 2002). Sections were washed with distilled water and incubated with a mixture of
192 0.005% TMB and 0.1% sodium cyanide for 20 min. H₂O₂ was added for 20 min, and the
193 reaction was stopped by washing in 0.01 M sodium acetate buffer. Alternate sections were
194 mounted on gelatin-coated slides within 6 h after TMB reaction. The next day, the sections were
195 dehydrated, defatted, and coverslipped. Slides containing TMB reacted sections were stored in
196 opaque boxes at 4°C to prevent degradation of TMB reaction product. All slides were coded and
197 analyzed without knowledge of treatment groups. Estimates of the number of retrogradely
198 labeled AT motoneurons was based on total bilateral counts done on adjacent sections at 100X
199 magnification. Every lumbar section was examined for labeled motoneurons, including several
200 sections beyond the rostral and caudal extent of AT motoneurons. Overall means and standard
201 errors are calculated and N = number of animals/group are reported in the figure captions.

202 ***Live imaging of endosomal transport in sciatic nerve axons.***

203 Endosomal trafficking in sciatic nerve axons of diseased (T-treated Tfm/TG) and healthy
204 (T-treated Tfm) male mice was assessed by directly monitoring the retrograde transport of
205 endosomes in living axons. CT B conjugated to Alexa Fluor 488 (CT-AF488; Molecular Probes,
206 USA, 10 µl of 0.2% in 0.9% saline containing 1% DMSO) was injected into the AT and
207 gastrocnemius muscles of isoflurane-anesthetized mice to label endosomes. Retrograde
208 movement of endosomes in living axons of explanted sciatic nerves was monitored four hours
209 after injection. During the 4 hour delay, mice were awake and mobile.

210 Mice were re-anesthetized with isoflurane to harvest the sciatic nerve. Explants (~10 mm
211 in length) were placed on coverglass, glued in place (VetBond 3M, USA) and covered with 37°C
212 oxygenated bicarbonate Ringer's solution (in mM: 135 NaCl, 5 KCl, 1 MgCl₂, 1.5 NaHCO₃, 1

213 Na₂PO₄, 2 CaCl₂, and 1.1 glucose, pH 7.2). The right sciatic nerve was harvested first and
214 recorded from while the left nerve remained *in situ* in the anesthetized mouse. There is no
215 evidence that transport in left and right nerves systematically differs nor that transport declines
216 over time (data not shown), consistent with previous findings (Kemp et al., 2011). Body
217 temperature was maintained using a heating pad for the 30 minutes between nerve harvests.
218 Once both nerves were harvested, the mouse was killed.

219

220 ***Live image acquisition and processing.***

221 Time-lapse movies of moving endosomes were made using an inverted LiveScan swept
222 field confocal microscope (Nikon Eclipse TE2000-E, Japan) equipped with a 60x PlanApo oil
223 immersion objective (1.4 NA), illuminated with the 488 nm line of a 150 mW argon laser (Melles
224 Griot), and recorded with a Photometrics CoolSNAP HQ2 camera (USA) using the NIS
225 elements software. Temperature of the sciatic nerve explant was maintained at 37°C by a ring
226 incubator. Less than 10 minutes after nerve harvest, recordings began, with two time-lapse
227 movies taken from the same explant within 30 minutes of harvest. Each movie was seven
228 minutes in length, comprising 211 images, with images captured every 2 sec at a 1 sec
229 exposure. Laser power and aperture settings were identical for all captured images. Scanning
230 for trafficking started at the center of the sciatic nerve segment and proceeded toward the distal
231 end of the nerve to reduce variability. Because of concerns about photobleaching, different
232 axons in the same explants were used for the two movies and the second movie was taken from
233 a region distal to the first. To minimize experimenter bias, video capture began when the first
234 moving endosome could be kept in focus.

235

236 ***Trafficking measures from kymographs.***

237 Time-lapse movies were converted into kymographs, single 2-dimensional images
238 showing the movement of endosomes (referred to as “endosomal traces”) along the length of an

239 axon as a function of time. To make kymographs, the resulting movies were opened in NIH
240 ImageJ as a 16 bit stack of images then rotated 90° counterclockwise. A 60 pixel wide length of
241 axon was then cropped, and using the 're-slice' option, sliced into 1 pixel width sections and z-
242 projected using the SUM option, which resulted in 32 bit 'raw' kymographs. The raw
243 kymographs were converted to 16 bits, and saved as tiff files. To facilitate visibility of transport
244 events, raw kymographs were opened in Adobe Photoshop (7.0 or CS2; USA), color inverted
245 and resampled to increase size by 500%, thus producing the kymographs used for analysis,
246 using ImageJ. We measured flux, net and instantaneous velocity, run length, and frequency of
247 trafficking perturbations (stalls, reversals and velocity changes) for retrogradely transporting
248 endosomes.

249 Endosomal flux is the number of retrogradely transporting endosomes in an axon per
250 unit of time and was determined by drawing a line through the center of the kymograph parallel
251 to the time axis and counting the number of endosomal traces that cross that line. The total
252 number of endosomes per kymograph was then divided by seven minutes (total time
253 represented on the kymograph) to estimate endosomal flux in number of endosomes/minute.
254 Such estimates were averaged across individual axons within a single animal to obtain a single
255 estimate of flux per mouse. Net velocity of retrogradely transported endosomes is the net
256 distance traveled by each endosome in the distal to proximal direction over time and included
257 stalls, reversals in direction and/or changes in velocity that might have occurred. Measures of
258 net velocity were obtained from kymographs by drawing a box around each endosomal trace
259 such that the far ends of the trace pass through opposite corners of the box. Height and width of
260 the box (in pixels) corresponding to length and time are used to calculate velocity
261 (microns/second) based on the following formula: $[\text{Distance (pixels)} \times 0.10526 \text{ (microns/pixel)} /$
262 $\text{Time (pixels)} \times \text{seconds per frame}]$. Net velocities of individual endosomal traces in a single
263 kymograph were then averaged to provide the mean estimate of net velocity/axon. These

264 estimates were then averaged across individual axons sampled within a single animal to obtain
265 a single estimate of net velocity per mouse.

266 Instantaneous velocity was measured by drawing a one pixel wide line parallel to the
267 time axis, bisecting the kymograph with respect to distance. For each endosomal trace crossing
268 the center line, a 20 pixel box was drawn around it, centering it with respect to the bisecting line,
269 with width and height of the box representing distance and time, respectively. The width of the
270 box (20 pixels) accounted for 6.6% (1.67 mm) of the total distance traveled and any continuous
271 velocity within it was considered instantaneous. The time it took to travel this short distance was
272 calculated based on the height of the box, which was adjusted so that its corners intersected the
273 most distal and proximal aspects of the trace. On rare occasions, perturbations in endosomal
274 velocity, including changes in speed, stalls and/or reversals, appeared within the box. In such
275 cases, the box was moved immediately distal to the trafficking perturbation or until the box
276 included a part of the endosomal trace that contained no trafficking perturbations. Instantaneous
277 velocity (microns/second) was calculated based on the same formula used for net velocity.
278 Measures of instantaneous velocity for each endosome were averaged within a single
279 kymograph and such estimates from two to four axons of the same mouse were averaged to
280 obtain a single estimate of instantaneous velocity per mouse.

281 We also assessed the frequency of trafficking perturbation events, which reflects the
282 efficiency by which endosomes are transported retrogradely. We counted the number of
283 trafficking perturbation events per trace, which included changes in velocity, stalls, and/or
284 reversals that lasted for \geq two seconds (Figure 1). Our measure of velocity changes was based
285 on visible changes in velocity in the kymograph without directly measuring changes in the slope
286 of the endosomal trace, indicating that subtle changes in velocity may have not been detected.
287 Stalls were defined as an endosome that was stationary for \geq 2 s. Stalling prevalence was
288 assessed by determining the number of stalls per endosomal trace and the proportion of traces

289 that had stalls. We also measured average run length, which was estimated by adding together
290 the total distance of endosomal transport observed in a kymograph and dividing this by the
291 number of stalls. As above, measures were averaged across multiple kymographs for each
292 animal, with N = number of animals per group for all statistical analyses. Data for reversals,
293 stalls, velocity changes, and overall trafficking perturbations are presented as a percentage of
294 total endosomes. Mean estimates of trafficking measures were based on 15-30 endosomal
295 traces per kymograph, with 2-4 kymographs per mouse and N = number of animals/group.
296 Analyses of kymographs were done by an experimenter blind to animal ID and genotype. Refer
297 to statistical table for description of data structure, statistical test used, and 95% confidence
298 intervals of data (Table 1).

299

Results

300 ***Activation of transgenic WT-AR in skeletal muscle fibers is sufficient for androgen-***
301 ***dependent deficits in both motor function and retrograde transport.***

302 We find that motor function based on forelimb grip strength of adult Tfm/TG males
303 rapidly declines during the five days of androgen treatment while motor function in Tfm-only
304 males remains stable and is unaffected by androgen (Figure 2A). After only 24 hours of
305 androgen exposure, motor function in Tfm/TG males is significantly reduced compared to Tfm-
306 only males (day 1 $p=0.002$) and continues to drop progressively during the next four days (day 2
307 $p=0.0004$, day 3 $p=0.0003$, day 4 $p=0.00001$, day 5 $p=0.00006$)^a, exhibiting the same time
308 course of demise as seen in T-treated myogenic TG females (Johansen et al., 2009). These
309 data also replicate previous results for Tfm/TG males (Johansen et al., 2011). Both Tfm and
310 Tfm/TG males without T treatment have T levels about 10 times lower than do adult WT males
311 (Johansen et al., 2011), suggesting that the low circulating level of T is why adult Tfm/TG males
312 do *not* develop motor dysfunction on their own.

313 Muscles of Tfm/TG mice and Tfm controls were injected with CT-HRP at the end of
314 treatment (5 days) to assess the efficiency of transport based on the number of retrogradely
315 labeled motoneurons. We find that motor-impaired Tfm/TG males have a significant deficit in the
316 number of retrogradely labeled motoneurons compared to Tfm controls (Figure 2B, $p=0.0027$)^b.
317 Interestingly, the number of labeled motoneurons for Tfm control males is comparable to that
318 previously reported for *gonadectomized* WT males who lack testicular androgens (Kemp et al.,
319 2011), with the number of retrogradely labeled motoneurons in both gonadally intact Tfm males
320 and gonadectomized WT males somewhat reduced compared to those of gonadally intact WT
321 males. It is possible that one of the normal roles of WT AR when activated by endogenous
322 androgens is to enhance the retrograde transport of cargo to motoneuronal cell bodies.

323 We also find that endosomal transport in axons of diseased Tfm/TG males was affected
324 when assessed directly in living axons *ex vivo* using video microscopy. Specifically, endosomal
325 flux ($p=0.0079$)^e, but not net velocity ($p=0.411$)^d, is significantly impaired in sciatic nerve axons
326 (Figure 2C, D), suggesting that deficits in flux may account for the reduced number of
327 retrogradely labeled motoneurons in diseased Tfm/TG mice. This pattern of results is also seen
328 in both chronically diseased myogenic TG males and acutely diseased myogenic TG females
329 (Kemp et al., 2011).

330 We also measured instantaneous velocity and trafficking perturbations and unexpectedly
331 detected a deficit in instantaneous velocity (Figure 3A, $p=0.0178$)^e, an outcome that was *not*
332 apparent in myogenic TG males (Kemp et al., 2011). These data suggest that endogenous WT-
333 AR may have protected against the effects of a toxic muscle AR on instantaneous velocity.
334 Altered instantaneous velocity in Tfm/TG males suggests defects in dynein function, a notion
335 not without precedence as another SBMA mouse model showed reduced dynein heavy chain
336 levels in the ventral spinal root (Katsuno et al., 2006). We also find a greater percentage of
337 endosomes show trafficking perturbations in diseased Tfm/Tg males (Figure 3B, $p=0.0387$)^f,

338 caused by more endosomes in diseased Tfm/TG males showing changes in velocity (Figure 3C,
 339 $p=0.0435$)^g and reversals (Figure 3D, $p=0.0314$)^h compared to endosomes in axons of healthy
 340 Tfm males. Surprisingly, although more endosomes tend to stall in diseased axons than in
 341 healthy axons, this difference was not significant (Figure 3E, $p=0.0955$)ⁱ. Likewise, while the
 342 mean run length of endosomes in Tfm/TG is shorter, it too was not significantly decreased
 343 compared to that of healthy Tfm males (Figure 3F, $p=0.2784$)^j. Together these data suggest that
 344 endogenous WT-AR may have protected against some of the effects of a toxic muscle AR on
 345 transport and converge on the conclusion that AR acting *only* in muscle fibers is sufficient to
 346 impair retrograde transport/trafficking of endosomes in motoneurons.

347

348 **Table 1. Statistical table.** Structure of data, statistical test used, and 95% confidence intervals
 349 are listed for each variable measured.

	Data Structure	Type of test	95% Confidence Interval for the mean Tfm (Lower bound, Upper bound); Tfm/TG (Lower bound, Upper bound)
^a Grip strength	Normal	Repeated measures ANOVA	Day 0: n/a
			Day 1: Tfm (84.72, 136.78); Tfm/TG (37.74, 79.06)
			Day 2: Tfm (69.78, 124.22); Tfm/TG (15.43, 49.37)
			Day 3: Tfm (60.88, 142.62); Tfm/TG (10.06, 30.34)
			Day 4: Tfm (82.57, 118.43); Tfm/TG (-6.59, 25.39)

			Day 5: Tfm (74.99, 113.01); Tfm/TG (-8.81, 31.61)
^b HRP filled motoneurons	Normal	Independent t-test	Tfm (93.81, 195.19); Tfm/TG (51.44, 90.96)
^c Flux	Normal	Independent t-test	Tfm (3.49, 8.16); Tfm/TG (2.22, 4.52)
^d Net velocity	Normal	Independent t-test	Tfm (0.25, 0.53); Tfm/TG (0.30, 0.45)
^e Instantaneous velocity	Normal	Independent t-test	Tfm (0.41, 0.86); Tfm/TG (0.34, 0.58)
^f Overall trafficking perturbations	Normal	Independent t-test	Tfm (3.46, 18.79); Tfm/TG (10.52, 34.11)
^g Velocity changes	Normal	Independent t-test	Tfm (1.12, 5.61); Tfm/TG (2.86, 11.61)
^h Reversals	Normal	Independent t-test	Tfm (3.10, 18.79); Tfm/TG (11.20, 34.10)
ⁱ Stalls	Normal	Independent t-test	Tfm (0.75, 8.92); Tfm/TG (4.53, 16.11)
^l Run length	Tfm group positively skewed (skewness: 2.198)	Independent t-test	Tfm (-444.43, 1881.98); Tfm/TG (41.77, 499.35)

350

351

352

Discussion

353 Here we demonstrate that retrograde axonal transport in motoneurons is impaired via
354 *non-cell autonomous* AR action in muscle. Myogenic contributions to SBMA were first
355 recognized in two different mouse models (Monks et al., 2007; Yu et al., 2006), where
356 myopathic changes were discovered in a knock-in model well before neuropathy and
357 transgenically overexpressed WT-AR *specifically* in muscle cells triggered SBMA-like symptoms
358 only in myogenic TG males, including a loss of ventral root axons. These unexpected findings
359 suggested that non-cell autonomous mechanisms originating in muscle could drive
360 pathogenesis in motoneurons in SBMA mice. We now find that AR in muscle is sufficient to
361 disrupt retrograde transport in the motoneurons which innervate diseased muscle. Previous
362 findings indicated that myogenic TG mice exhibit perturbed axonal transport compared to WT
363 littermates (Kemp et al., 2011). However, such TG mice also had AR in other cell types due to
364 expression of the endogenous gene, leaving open the possibility that endogenous AR in the
365 motoneurons and/or in other cell types was responsible for the transport deficits found in this
366 model. Thus, we asked whether the effects of TG AR in muscle fibers depend on endogenous
367 AR in other cell types by assessing axonal transport in myogenic TG males that also have the
368 *Tfm* allele of the endogenous *AR* gene (*Tfm*/TG males), thus eliminating all functional AR from
369 the endogenous gene. Consequently, such *Tfm*/TG males had functional AR *only* in skeletal
370 muscle fibers due to expression of the AR transgene. We found that diseased *Tfm*/TG males
371 showed comparable deficits in the number of retrogradely labeled motoneurons and in
372 endosomal flux as previously reported for diseased TG males on a WT AR background (Kemp
373 et al., 2011), indicating that AR acts solely in muscle fibers to perturb retrograde transport in
374 motoneurons.

375 As expected, *Tfm*/TG males exhibited androgen-dependent motor dysfunction,
376 replicating a previous finding from this same mouse model showing that such dysfunction is fully

377 reversible when androgen treatment ceases (Johansen et al., 2011; Johansen et al., 2009;
378 Monks et al., 2007; Figure 2A) and consistent with the phenotype of SBMA mouse models
379 expressing a CAG expanded AR allele (Chevalier-Larsen et al., 2004; Katsuno et al., 2002;
380 Renier et al., 2014; Sopher et al., 2004; Yu et al., 2006). Such mice also showed a striking
381 deficit in the number of retrogradely labeled motoneurons compared to non-diseased Tfm male
382 controls (Figure 2B), correlating with the deficit in motor function (Figure 2A). Interestingly, the
383 magnitude (~50%) of the labeling deficit in Tfm/TG males is comparable to that previously
384 reported for both chronically diseased myogenic TG males and acutely diseased myogenic TG
385 females (Kemp et al., 2011), indicating that TG AR in muscle, when activated by androgens,
386 rapidly perturbs the uptake/retrograde transport of CT-HRP by motoneuronal axons
387 independent of AR expressed by the native gene, including that in motoneurons and/or other
388 cell types.

389 Strong evidence argues that the deficit in axonal transport exhibited by androgen-treated
390 Tfm/TG males is largely comparable to that previously observed in TG-only males and females.
391 Notably, deficits in CT-HRP staining and grip strength are apparent after only 24h of T-treatment
392 in TG-only females (Kemp et al., 2011), the time-point at which Tfm/TG males, given the same
393 T-treatment, show deficits in grip strength. Moreover, CT-HRP transport recovers fully in
394 chronically symptomatic TG males that have been castrated, as does motor function in
395 symptomatic Tfm/TG males following T removal (Johansen et al., 2011; Kemp et al., 2011). It is
396 clear that the transgene alone without androgen stimulation is not sufficient to induce transport
397 dysfunction, in parallel with the effect of the transgene on motor function, since castrated TG
398 males and untreated TG females show deficits in neither motor function nor axonal transport
399 (Kemp et al., 2011). Unfortunately, any direct comparison between TG and Tfm/TG males in
400 disease traits would be confounded by long term versus short term effects of disease. TG-only
401 males are exposed throughout life to endogenous male levels of androgens, causing secondary
402 effects of disease due to its chronic nature in TG-only males. On the other hand, Tfm/TG males

403 like TG-only females, lack endogenous male levels of androgens postnatally, and only express
404 an acute disease phenotype when provided with exogenous androgens. In sum, the defects in
405 transport and motor dysfunction induced by T treatment of Tfm/TG males, who like TG-only
406 males and females, express the disease-causing AR allele *only* in muscle fibers, is comparable
407 to what is seen in TG-only males and females in which *both* motor function and axonal transport
408 are disrupted only in the presence of male levels of androgens.

409 Evidence strongly argues that the deficit found in the number of retrogradely labeled
410 motoneurons is not caused by a net loss of motoneurons. Cell counts of motoneuronal cell
411 bodies in Nissl stained sections of the spinal cord show no evidence of motoneuronal loss in the
412 myogenic TG model (Johansen et al., 2009; Monks et al., 2007). Moreover, extending CT
413 transport time to 24 hours rather than the 12 hours used here eliminates the deficit in retrograde
414 labeling of motoneurons (Kemp et al., 2011). Notably, defects in axonal transport observed here
415 are not likely due to secondary effects of disease since deficits in CT-HRP transport occur just
416 24h after the commencement of T-treatment in female TG mice (Kemp et al., 2011) who display
417 the same time-course of deterioration as the inducible Tfm/TG model used here. Moreover, no
418 muscle atrophy is apparent in 5 day-treated TG females, despite their displaying severe motor
419 impairment and a loss of muscle force that does not involve a loss of muscle mass (Oki et al.,
420 2013). Additionally, no dying-back of the motoneuron occurs in even chronically diseased TG
421 males, as all endplates are contacted by a motor nerve terminal (Kemp et al., 2011). Thus,
422 deficits in axonal transport and not neuronal loss nor muscle atrophy correlate with motor
423 dysfunction, suggesting that axonal transport dysfunction may contribute to early losses in
424 motor function and ultimately motoneuron death in SBMA.

425 This deficit in retrograde labeling of motoneurons may be due to a number of factors,
426 including dysfunction originating in the distal most aspect of the axon, the synaptic nerve
427 terminal, where material is first taken up, sorted, and packaged into vesicles for either local
428 recycling or retrograde transport to the motoneuronal cell bodies. Deficits could also originate in

429 more proximal aspects of the axon. Transport of cargo in these two axonal compartments
430 depends on different transport machinery, with local transport of cargo in the synaptic nerve
431 terminal moved along actin by specialized myosin, whereas long distance transport of cargo
432 toward motoneuronal cell bodies is moved along microtubules by dynein and the motor-
433 associated protein complex dynactin (Chevalier-Larsen & Holzbaur, 2006). Our first-level
434 analysis of endosomal transport in living axons of diseased Tfm/TG indicated that endosomal
435 flux, but not net velocity, was perturbed in Tfm/TG males, as found previously in chronically
436 diseased myogenic males and acutely diseased myogenic females (Kemp et al., 2011). Thus,
437 fewer labeled endosomes than normal move along the diseased axon per unit of time, offering
438 an explanation for why fewer motoneurons in diseased Tfm/TG mice are retrogradely labeled
439 after 12 hours of CT transport. Such a deficit in flux suggests that the early endocytotic pathway
440 in the nerve terminal is susceptible to non-cell autonomous regulation, with disease signals
441 originating in muscle perturbing some aspect of this presynaptic pathway, including possibly the
442 uptake, local sorting, packaging/fusion, and/or movement of CT-containing cargo within the
443 synaptic nerve terminal. Moreover, the nerve terminal exhibits accumulation of neurofilament in
444 SBMA patients, further linking the distal axon to defects in transport (Katsuno et al., 2006).
445 Nevertheless, which of these processes is affected is not clear and would require direct
446 monitoring of endocytosis in synaptic nerve endings to determine.

447 While net velocity was *not* affected by disease in Tfm/TG males, paradoxically
448 instantaneous velocity was, counter to previous findings reported for myogenic TG males (Kemp
449 et al., 2011). A deficit in instantaneous velocity means that when endosomes are in motion, they
450 move slower in diseased axons than in healthy axons, raising questions about whether AR in
451 muscle can also cause defects in the retrograde motor dynein (Alper et al., 2013). A possible
452 explanation for dynein dysfunction *per se* is suggested by a report from Ramzan et al. (2015).
453 Using Cre-lox technology to drive expanded polyglutamine AR expression specifically in muscle
454 fibers (MyoAR), they found reduced nitrotyrosine staining in motoneurons (Ramzan et al.,

455 2015). These data suggest a loss of oxidative homeostasis in motoneurons triggered by
456 diseased muscle can in turn impair dynein. In fact, dynein heavy chain is reduced in ventral
457 spinal root of symptomatic AR97Q SBMA mice, but only in later stages of disease (Katsuno et
458 al., 2006).

459 The effect of disease on instantaneous velocity in Tfm/TG males is reminiscent of
460 previous findings in a knock-in model of SBMA, also involving a deficit in instantaneous velocity
461 (Kemp et al., 2011). While these data suggested that mutant AR expressed in motoneurons can
462 cause defects in dynein/dynactin function in a cell autonomous fashion, the current data suggest
463 an additional hypothesis that endogenous (WT) AR in motoneurons of TG males may have
464 protected against the toxic effects of muscle TG AR on instantaneous velocity. Knock-in males
465 would not have this protection since every cell that expresses AR in this model, expresses only
466 the mutant AR allele. This suggestion is consistent with previous findings that endogenous WT
467 AR can blunt the toxicity of a disease-causing TG AR in a different SBMA model (Thomas et al.,
468 2006). It is also possible that endogenous AR in muscle could have a protective role, but this
469 scenario seems less parsimonious. Finally, while AR aggregates perturbed axonal transport in
470 one SBMA cell model (Piccioni et al., 2002), this cannot explain the defects seen in the current
471 TG model as AR aggregates do not occur in myogenic mice (Monks et al., 2007), nor do they
472 occur in axons of other SBMA models in which axonal transport defects have been found
473 (Katsuno et al., 2006; Szebenyi et al., 2003).

474 We also found that retrogradely transporting endosomes in diseased axons had a higher
475 overall incidence of trafficking perturbations, with more endosomes in axons of Tfm/TG males
476 showing reversals, stalls, and velocity changes than endosomes in axons of healthy Tfm males
477 (Figure 3). Such “error” events reflect reduced processivity. An important regulator of
478 processivity is the motor-associated protein dynactin (King & Schroer, 2000). In fact, dynactin is
479 reduced in motoneurons of SBMA patients and in a mouse model of SBMA in which the disease
480 allele is globally expressed and shows early defects in axonal transport (Katsuno et al., 2006),

481 suggesting it is likely to also be perturbed in the myogenic model. That transport of endosomes
482 in axons of diseased Tfm/TG males is less efficient suggests that dynactin function is also
483 perturbed in a *non-cell autonomous* manner by diseased muscle. The run length of endosomes
484 in axons of diseased Tfm/Tg males is also shorter than in axons of healthy Tfm axons,
485 consistent with reduced processivity, though this difference is not significant, perhaps because
486 of the increased error variance seen in healthy Tfm controls. Nonetheless, together these data
487 suggest that signals from diseased muscle can instigate defects in the core transport machinery
488 involving the retrograde motor and its associated proteins although the effect of diseased
489 muscle on retrograde transport seems to lie predominantly in the motor synapse where cargo is
490 first taken up and packaged. While the current study represents a small step toward recognizing
491 the potential role of non-cell autonomous regulators of axonal transport, this possibility is
492 sufficiently important to merit further investigation.

493 The fact that instantaneous velocity but not net velocity is perturbed in Tfm/TG diseased
494 males suggests that compensation occurred. One possible explanation is that while reversals
495 are more common in diseased axons, perhaps the distance traversed in the wrong direction is
496 less in diseased than healthy axons. Regardless of the explanation for the apparent discrepancy
497 in instantaneous versus net velocity, the current findings raise the possibility that dynein and
498 dynactin, essential in the retrograde transport of cargo, are each susceptible to non-cell
499 autonomous regulation by the muscle. While there is precedence that both dynein and dynactin
500 are impaired in models of SBMA (Katsuno et al., 2006; Szebenyi et al., 2003), the current data
501 are the first to suggest that such defects in motor proteins could be caused via a non-cell
502 autonomous mechanism.

503 How might action of a toxic AR in muscle perturb axonal transport in the motoneurons?
504 One attractive scenario is the loss of muscle-derived trophic factors. Skeletal muscle releases
505 many kinds of trophic factors that can act on receptors in motor nerve terminals to promote
506 healthy cell function. Diseased muscle from various SBMA mouse models exhibits deficits in

507 multiple trophic factors, including brain-derived neurotrophic factor (BDNF), glial cell line-derived
508 factor, insulin-like growth factor 1, neurotrophin-4 (NT-4), and vascular endothelial growth factor
509 (VEGF) (Halievski et al., 2015; Mo et al., 2010; Monks et al., 2007; Sopher et al., 2004; Yu et
510 al., 2006). Moreover, replenishing the supply of such neurotrophic factors can reverse disease-
511 related deficits in axonal transport in models of motoneuron/neuromuscular disease. For
512 example, delivery of CNTF, BDNF, or NT-3 to muscle improves retrograde transport in the
513 *progressive motor neuronopathy* mouse model (Sagot et al., 1998). Additionally, treating
514 diseased muscles of myogenic TG SBMA females with VEGF reverses a disease-related deficit
515 in retrograde labeling of motoneurons and endosomal flux (Kemp et al., 2011). These data are
516 compelling precedence for a cause-effect relationship between muscle-supplied neurotrophic
517 factors and retrograde transport in motoneurons.

518 Loss of such trophic support from target musculature could lead to defective transport in
519 at least two ways. First, lack of trophic factor signaling might mean a loss of survival signaling,
520 leaving the cell deprived of needed resources for proper maintenance of axonal transport
521 (Chowdary et al., 2012). Alternatively, local neurotrophic signaling may be needed for
522 endocytosis *per se*, since VEGF can reverse a deficit in flux (Kemp et al., 2011). Internalization
523 of the neurotrophin-bound Trk receptor requires PI3K signaling to recruit Rab5 (Christoforidis et
524 al., 1999; also see Harrington & Ginty, 2013 for review). Since internalization and sorting of the
525 CT receptor GM1 also depends on Rab5 (Pelkmans et al., 2004), neurotrophic factors could
526 enhance endocytosis through this pathway. Once internalized, Trk signaling also leads to
527 phosphorylation of dynein intermediate chains through the MAPK/ERK pathway to enhance
528 binding of dynein to Trk-activated signaling endosomes (Mitchell et al., 2012). Defects in this
529 pathway could explain the deficit in flux as well as the reduced efficiency of transport in
530 diseased axons. In short, muscle-derived neurotrophic factors are a strong candidate for how
531 diseased muscle might disrupt the uptake and/or retrograde transport of cargo in motoneuronal

532 axons of SBMA mice (see Figure 4 for a proposed model). While data are scant, the relevance
533 of these data to SBMA in humans is likely (Katsuno et al., 2006).

534 While considerable attention has recently been redirected to muscle, recent work also
535 supports the idea that mutant AR acting in motoneurons contributes to SBMA pathogenesis
536 (Ramzan et al., 2015; Sahashi et al., 2015). Given that both motoneurons and muscle normally
537 express AR, and that motoneurons and muscles are interdependent, it would not be surprising if
538 the symptoms of SBMA reflects a complex interplay of mutant AR acting in both motoneurons
539 and skeletal muscles, if not in other cell types too. The important task before us is to better
540 understand where and how mutant AR acts to cause disease and to sort out primary effects of
541 AR from secondary effects of disease. AR acting in muscle to impair axonal transport may be
542 one such early pathogenic event leading to widespread neuromuscular dysfunction.

543 Figure Captions

544 **Figure 1. Representative kymograph showing various trafficking perturbations**

545 **measured.** Endosomal traces are seen as dark irregular lines that typically slope downward
546 from right to left, indicating the time it takes for a given endosome to traverse a given length
547 (25.26 μm) of axon. Note that the slope of the trace can change over time, going from a
548 downward slope to one that is vertical (parallel to the time axis) indicating a stall (1), to less
549 severe changes in slope (2 versus 3), with the steeper downward slope (3) indicating a transient
550 increase in endosomal velocity. A negative slope in an endosomal trace (4) indicates that the
551 endosome transiently reversed its direction of movement. The shown kymograph is taken from
552 a healthy Tfm male.

553 **Figure 2. Adult male mice with functional AR only in skeletal muscle fibers (Tfm/TG)**

554 **show defects in motor function, retrograde transport, and endosomal trafficking. (A)**

555 Myogenic TG male mice with a mutant allele (*testicular feminization mutation*, Tfm) of the
556 endogenous AR gene (Tfm/TG) show an androgen-dependent loss of grip strength, with grip
557 strength dropping to basement within 4 days of testosterone (T) exposure. Both groups of males
558 were treated with exogenous T given their negligible levels of endogenous androgen. Note that
559 the grip strength of Tfm controls who lack functional AR is unaffected by T. **(B)** The number of
560 anterior tibialis motoneurons filled with CT-HRP after 12 hrs of retrograde transport is
561 significantly reduced in diseased Tfm/TG males compared to healthy Tfm controls, indicating
562 that transgenic AR acting in muscle fibers induces defects in retrograde transport, independent
563 of endogenous wild-type AR in motoneurons and elsewhere. **(C, D)** Such Tfm/TG mice show
564 deficits in flux, but not net velocity, after 5 days of T treatment, comparable to reported results
565 from TG males on a wild-type background (Kemp et al., 2011). The current data reinforce the
566 idea that muscle AR instigates a disease process that retrogradely impairs endosomal
567 trafficking in motoneurons, possibly by perturbing aspects of the early endocytotic pathway.

568 Graphs represent mean \pm SEM (A, B: N = 4-5/group; C, D: N = 6/group). A repeated measures
569 ANOVA indicated a grip strength by group interaction, and further revealed an effect of time on
570 grip strength only for the Tfm/TG genotype. * indicates significant differences ($p < 0.05$) between
571 groups based on a one-way ANOVA (A) and independent t-test (B - D).

572 **Figure 3. Androgen activated AR in skeletal muscle fibers perturbs trafficking kinetics of**
573 **retrogradely transporting endosomes.** Based on live imaging of fluorescently-labeled
574 trafficking endosomes in sciatic nerve axons of Tfm and Tfm/TG males, we find that the
575 instantaneous velocity (**A**) of transporting endosomes is significantly decreased in diseased
576 Tfm/TG males compared to Tfm control males. Endosomes in motor-impaired Tfm/TG males
577 also show elevated levels of trafficking perturbations overall (**B**), including an increased
578 tendency to show velocity changes (**C**), reversals (**D**) and stalls (**E**). The average run length (**F**)
579 of retrogradely transporting endosomes was also shorter in diseased Tfm/TG males, but this
580 difference was not significant, perhaps due to the larger error variance in run length for Tfm
581 males. Because Tfm and Tfm/TG normally have very low levels of circulating androgens, males
582 used in this study were treated with testosterone, mimicking normal male levels of androgens.
583 Such trafficking perturbations demonstrate that non-cell autonomous mechanisms from skeletal
584 muscle can impair trafficking machinery in the axon proper, possibly perturbing the retrograde
585 motor dynein and its associated dynactin complex. Graphs represents mean \pm SEM (A-F: N =
586 6/group) and * indicates significant differences ($p < 0.05$) between groups based on independent
587 t-test.

588 **Figure 4. Proposed model of non-cell autonomous influence of muscle on motoneuronal**
589 **axonal transport.** In the healthy neuromuscular system, neurotrophic factors produced and
590 released from skeletal muscle support motoneuronal health and survival. SBMA skeletal muscle
591 is deficient in neurotrophic factors, which may lead to reduced endocytosis in motoneurons,
592 which may manifest as reduced retrograde transport of cholera toxin and reduced endosomal

593 flux, as observed in the present study. Therapies aimed at increasing muscle-derived
594 neurotrophic factors may remedy defective axonal transport and ameliorate disease symptoms.
595

596

References

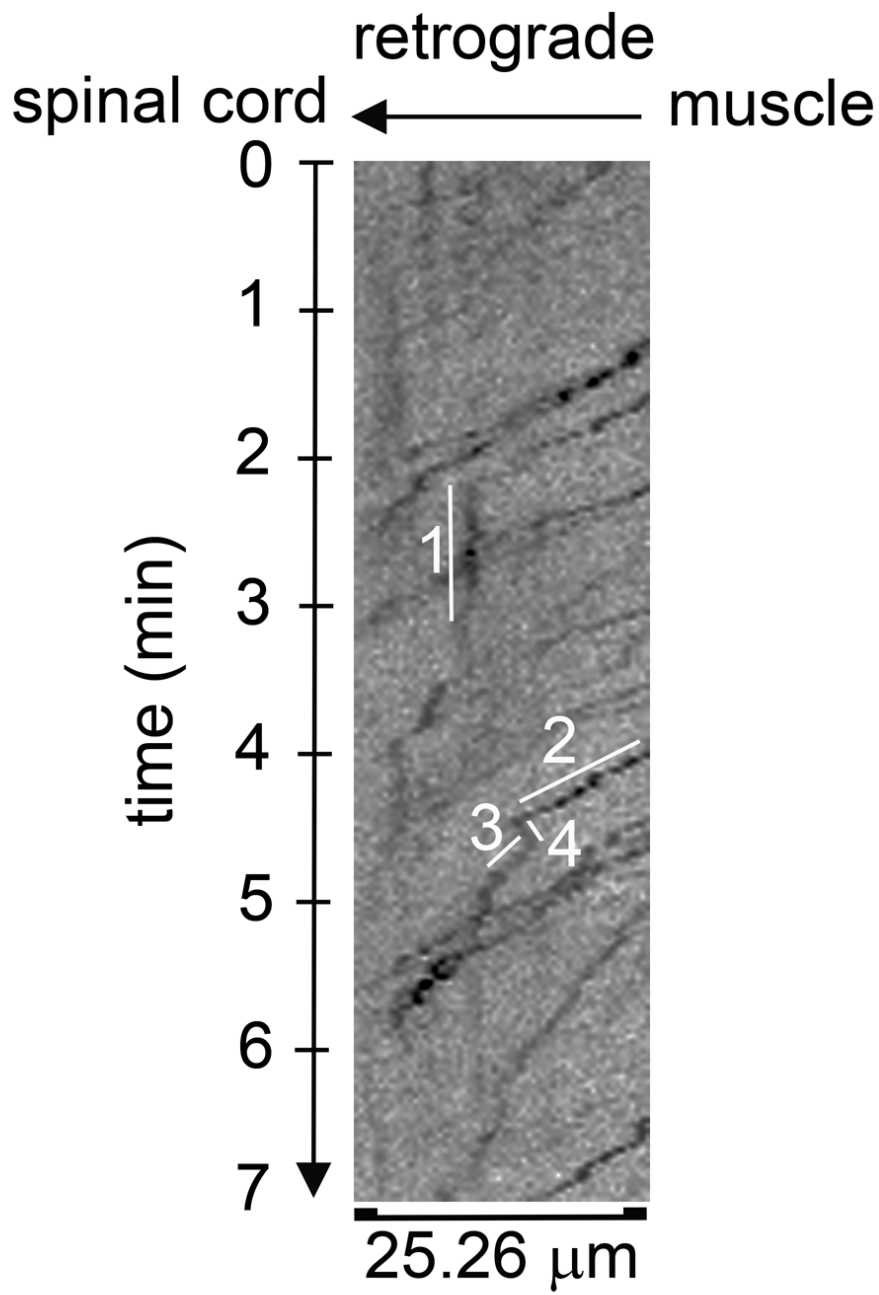
597

- 598 Alper, J. D., Tovar, M., & Howard, J. (2013) Displacement-weighted velocity analysis of gliding assays
599 reveals that *Chlamydomonas* axonemal dynein preferentially moves conspecific microtubules.
600 *Biophys. J.* 104:1989-1998. doi: 10.1016/j.bpj.2013.03.041
- 601 Baniahmad, A. (2015) Inhibition of the Androgen Receptor by Antiandrogens in Spinobulbar Muscle
602 Atrophy. *J. Mol. Neurosci.* doi: 10.1007/s12031-015-0681-8
- 603 Chevalier-Larsen, E., & Holzbaur, E. L. (2006) Axonal transport and neurodegenerative disease. *Biochim.*
604 *Biophys. Acta* 1762:1094-1108. doi: 10.1016/j.bbadis.2006.04.002
- 605 Chevalier-Larsen, E. S., O'Brien, C. J., Wang, H., Jenkins, S. C., Holder, L., Lieberman, A. P., & Merry, D. E.
606 (2004) Castration restores function and neurofilament alterations of aged symptomatic males in
607 a transgenic mouse model of spinal and bulbar muscular atrophy. *J. Neurosci.* 24:4778-4786.
608 doi: 10.1523/JNEUROSCI.0808-04.2004
- 609 Chowdhury, P. D., Che, D. L., & Cui, B. (2012) Neurotrophin signaling via long-distance axonal transport.
610 *Annual review of physical chemistry* 63:571-594. doi: 10.1146/annurev-physchem-032511-
611 143704
- 612 Christoforidis, S., Miaczynska, M., Ashman, K., Wilm, M., Zhao, L., Yip, S. C., Waterfield, M. D., Backer, J.
613 M., & Zerial, M. (1999) Phosphatidylinositol-3-OH kinases are Rab5 effectors. *Nat. Cell Biol.*
614 1:249-252. doi: 10.1038/12075
- 615 De Vos, K. J., Grierson, A. J., Ackerley, S., & Miller, C. C. (2008) Role of axonal transport in
616 neurodegenerative diseases. *Annu. Rev. Neurosci.* 31:151-173. doi:
617 10.1146/annurev.neuro.31.061307.090711
- 618 Goldstein, J. L., & Wilson, J. D. (1972) Studies on the pathogenesis of the pseudohermaphroditism in the
619 mouse with testicular feminization. *J. Clin. Invest.* 51:1647-1658. doi: 10.1172/JCI106966
- 620 Halievski, K., Henley, C. L., Domino, L., Poort, J. E., Fu, M., Katsuno, M., Adachi, H., Sobue, G., Breedlove,
621 S. M., & Jordan, C. L. (2015) Androgen-dependent loss of muscle BDNF mRNA in two mouse
622 models of SBMA. *Exp. Neurol.* 269:224-232. doi: 10.1016/j.expneurol.2015.04.013
- 623 Hamburger, V., & Levi-Montalcini, R. (1949) Proliferation, differentiation and degeneration in the spinal
624 ganglia of the chick embryo under normal and experimental conditions. *The Journal of*
625 *experimental zoology* 111:457-501.
- 626 Harrington, A. W., & Ginty, D. D. (2013) Long-distance retrograde neurotrophic factor signalling in
627 neurons. *Nat. Rev. Neurosci.* 14:177-187. doi: 10.1038/nrn3253
- 628 He, W. W., Kumar, M. V., & Tindall, D. J. (1991) A frame-shift mutation in the androgen receptor gene
629 causes complete androgen insensitivity in the testicular-feminized mouse. *Nucleic Acids Res.*
630 19:2373-2378.
- 631 Ilieva, H., Polymenidou, M., & Cleveland, D. W. (2009) Non-cell autonomous toxicity in
632 neurodegenerative disorders: ALS and beyond. *J. Cell Biol.* 187:761-772. doi:
633 10.1083/jcb.200908164
- 634 Johansen, J. A., Troxell-Smith, S. M., Yu, Z., Mo, K., Monks, D. A., Lieberman, A. P., Breedlove, S. M., &
635 Jordan, C. L. (2011) Prenatal flutamide enhances survival in a myogenic mouse model of spinal
636 bulbar muscular atrophy. *Neurodegener Dis* 8:25-34. doi: 10.1159/000313682
- 637 Johansen, J. A., Yu, Z., Mo, K., Monks, D. A., Lieberman, A. P., Breedlove, S. M., & Jordan, C. L. (2009)
638 Recovery of function in a myogenic mouse model of spinal bulbar muscular atrophy. *Neurobiol*
639 *Dis* 34:113-120. doi: 10.1016/j.nbd.2008.12.009
- 640 Jordan, C. L., & Lieberman, A. P. (2008) Spinal and bulbar muscular atrophy: a motoneuron or muscle
641 disease? *Curr Opin Pharmacol* 8:752-758. doi: 10.1016/j.coph.2008.08.006

- 642 Katsuno, M., Adachi, H., Kume, A., Li, M., Nakagomi, Y., Niwa, H., Sang, C., Kobayashi, Y., Doyu, M., &
643 Sobue, G. (2002) Testosterone reduction prevents phenotypic expression in a transgenic mouse
644 model of spinal and bulbar muscular atrophy. *Neuron* 35:843-854.
- 645 Katsuno, M., Adachi, H., Minamiyama, M., Waza, M., Tokui, K., Banno, H., Suzuki, K., Onoda, Y., Tanaka,
646 F., Doyu, M., & Sobue, G. (2006) Reversible disruption of dynactin 1-mediated retrograde axonal
647 transport in polyglutamine-induced motor neuron degeneration. *J. Neurosci.* 26:12106-12117.
648 doi: 10.1523/JNEUROSCI.3032-06.2006
- 649 Katsuno, M., Tanaka, F., Adachi, H., Banno, H., Suzuki, K., Watanabe, H., & Sobue, G. (2012)
650 Pathogenesis and therapy of spinal and bulbar muscular atrophy (SBMA). *Prog. Neurobiol.*
651 99:246-256. doi: 10.1016/j.pneurobio.2012.05.007
- 652 Kemp, M. Q., Poort, J. L., Baqri, R. M., Lieberman, A. P., Breedlove, S. M., Miller, K. E., & Jordan, C. L.
653 (2011) Impaired motoneuronal retrograde transport in two models of SBMA implicates two sites
654 of androgen action. *Hum. Mol. Genet.* 20:4475-4490. doi: 10.1093/hmg/ddr380
- 655 King, S. J., & Schroer, T. A. (2000) Dynactin increases the processivity of the cytoplasmic dynein motor.
656 *Nat. Cell Biol.* 2:20-24. doi: 10.1038/71338
- 657 La Spada, A. R., Wilson, E. M., Lubahn, D. B., Harding, A. E., & Fischbeck, K. H. (1991) Androgen receptor
658 gene mutations in X-linked spinal and bulbar muscular atrophy. *Nature* 352:77-79. doi:
659 10.1038/352077a0
- 660 Malik, B., Nirmalanathan, N., Bilsland, L. G., La Spada, A. R., Hanna, M. G., Schiavo, G., Gallo, J. M., &
661 Greensmith, L. (2011) Absence of disturbed axonal transport in spinal and bulbar muscular
662 atrophy. *Hum. Mol. Genet.* 20:1776-1786. doi: 10.1093/hmg/ddr061
- 663 Mitchell, D. J., Blasier, K. R., Jeffery, E. D., Ross, M. W., Pullikuth, A. K., Suo, D., Park, J., Smiley, W. R., Lo,
664 K. W., Shabanowitz, J., Deppmann, C. D., Trinidad, J. C., Hunt, D. F., Catling, A. D., & Pfister, K. K.
665 (2012) Trk activation of the ERK1/2 kinase pathway stimulates intermediate chain
666 phosphorylation and recruits cytoplasmic dynein to signaling endosomes for retrograde axonal
667 transport. *J. Neurosci.* 32:15495-15510. doi: 10.1523/JNEUROSCI.5599-11.2012
- 668 Mo, K., Razak, Z., Rao, P., Yu, Z., Adachi, H., Katsuno, M., Sobue, G., Lieberman, A. P., Westwood, J. T., &
669 Monks, D. A. (2010) Microarray analysis of gene expression by skeletal muscle of three mouse
670 models of Kennedy disease/spinal bulbar muscular atrophy. *PLoS One* 5:e12922. doi:
671 10.1371/journal.pone.0012922
- 672 Monks, D. A., Johansen, J. A., Mo, K., Rao, P., Eagleson, B., Yu, Z., Lieberman, A. P., Breedlove, S. M., &
673 Jordan, C. L. (2007) Overexpression of wild-type androgen receptor in muscle recapitulates
674 polyglutamine disease. *Proceedings of the National Academy of Sciences of the United States of*
675 *America* 104:18259-18264. doi: 10.1073/pnas.0705501104
- 676 Morfini, G., Pigino, G., Szebenyi, G., You, Y., Pollema, S., & Brady, S. T. (2006) JNK mediates pathogenic
677 effects of polyglutamine-expanded androgen receptor on fast axonal transport. *Nat. Neurosci.*
678 9:907-916. doi: 10.1038/nn1717
- 679 Morfini, G. A., Burns, M., Binder, L. I., Kanaan, N. M., LaPointe, N., Bosco, D. A., Brown, R. H., Jr., Brown,
680 H., Tiwari, A., Hayward, L., Edgar, J., Nave, K. A., Garberrn, J., Atagi, Y., Song, Y., Pigino, G., &
681 Brady, S. T. (2009) Axonal transport defects in neurodegenerative diseases. *J. Neurosci.*
682 29:12776-12786. doi: 10.1523/JNEUROSCI.3463-09.2009
- 683 Murphy, L., & O'Shaughnessy, P. J. (1991) Testicular steroidogenesis in the testicular feminized (Tfm)
684 mouse: loss of 17 alpha-hydroxylase activity. *J. Endocrinol.* 131:443-449.
- 685 Navarro, X., Vivo, M., & Valero-Cabre, A. (2007) Neural plasticity after peripheral nerve injury and
686 regeneration. *Prog. Neurobiol.* 82:163-201. doi: 10.1016/j.pneurobio.2007.06.005
- 687 Oki, K., Wiseman, R. W., Breedlove, S. M., & Jordan, C. L. (2013) Androgen receptors in muscle fibers
688 induce rapid loss of force but not mass: implications for spinal bulbar muscular atrophy. *Muscle*
689 *Nerve* 47:823-834.

- 690 Park, J. J., Zup, S. L., Verhovshek, T., Sengelaub, D. R., & Forger, N. G. (2002) Castration reduces
691 motoneuron soma size but not dendritic length in the spinal nucleus of the bulbocavernosus of
692 wild-type and BCL-2 overexpressing mice. *J. Neurobiol.* 53:403-412. doi: 10.1002/neu.10103
- 693 Pelkmans, L., Burli, T., Zerial, M., & Helenius, A. (2004) Caveolin-stabilized membrane domains as
694 multifunctional transport and sorting devices in endocytic membrane traffic. *Cell* 118:767-780.
695 doi: 10.1016/j.cell.2004.09.003
- 696 Piccioni, F., Pinton, P., Simeoni, S., Pozzi, P., Fascio, U., Vismara, G., Martini, L., Rizzuto, R., & Poletti, A.
697 (2002) Androgen receptor with elongated polyglutamine tract forms aggregates that alter
698 axonal trafficking and mitochondrial distribution in motor neuronal processes. *FASEB J.* 16:1418-
699 1420. doi: 10.1096/fj.01-1035fje
- 700 Ramzan, F., McPhail, M., Rao, P., Mo, K., Halievski, K., Swift-Gallant, A., Mendoza-Viveros, L., Cheng, H.
701 Y., & Monks, D. A. (2015) Distinct Etiological Roles for Myocytes and Motor Neurons in a Mouse
702 Model of Kennedy's Disease/Spinobulbar Muscular Atrophy. *J. Neurosci.* 35:6444-6451. doi:
703 10.1523/JNEUROSCI.3599-14.2015
- 704 Renier, K. J., Troxell-Smith, S. M., Johansen, J. A., Katsuno, M., Adachi, H., Sobue, G., Chua, J. P., Sun Kim,
705 H., Lieberman, A. P., Breedlove, S. M., & Jordan, C. L. (2014) Antiandrogen flutamide protects
706 male mice from androgen-dependent toxicity in three models of spinal bulbar muscular atrophy.
707 *Endocrinology* 155:2624-2634. doi: 10.1210/en.2013-1756
- 708 Sagot, Y., Rosse, T., Vejsada, R., Perrelet, D., & Kato, A. C. (1998) Differential effects of neurotrophic
709 factors on motoneuron retrograde labeling in a murine model of motoneuron disease. *J.*
710 *Neurosci.* 18:1132-1141.
- 711 Sahashi, K., Katsuno, M., Hung, G., Adachi, H., Kondo, N., Nakatsuji, H., Tohnai, G., Iida, M., Bennett, C.
712 F., & Sobue, G. (2015) Silencing neuronal mutant androgen receptor in a mouse model of spinal
713 and bulbar muscular atrophy. *Hum. Mol. Genet.* 24:5985-5994. doi: 10.1093/hmg/ddv300
- 714 Sambataro, F., & Pennuto, M. (2012) Cell-autonomous and non-cell-autonomous toxicity in
715 polyglutamine diseases. *Prog. Neurobiol.* 97:152-172. doi: 10.1016/j.pneurobio.2011.10.003
- 716 Sopher, B. L., Thomas, P. S., Jr., LaFevre-Bernt, M. A., Holm, I. E., Wilke, S. A., Ware, C. B., Jin, L. W.,
717 Libby, R. T., Ellerby, L. M., & La Spada, A. R. (2004) Androgen receptor YAC transgenic mice
718 recapitulate SBMA motor neuronopathy and implicate VEGF164 in the motor neuron
719 degeneration. *Neuron* 41:687-699.
- 720 Szebenyi, G., Morfini, G. A., Babcock, A., Gould, M., Selkoe, K., Stenoi, D. L., Young, M., Faber, P. W.,
721 MacDonald, M. E., McPhaul, M. J., & Brady, S. T. (2003) Neuropathogenic forms of huntingtin
722 and androgen receptor inhibit fast axonal transport. *Neuron* 40:41-52.
- 723 Thomas, P. S., Jr., Fraley, G. S., Damian, V., Woodke, L. B., Zapata, F., Sopher, B. L., Plymate, S. R., & La
724 Spada, A. R. (2006) Loss of endogenous androgen receptor protein accelerates motor neuron
725 degeneration and accentuates androgen insensitivity in a mouse model of X-linked spinal and
726 bulbar muscular atrophy. *Hum. Mol. Genet.* 15:2225-2238. doi: 10.1093/hmg/ddl148
- 727 Yu, Z., Dadgar, N., Albertelli, M., Gruis, K., Jordan, C., Robins, D. M., & Lieberman, A. P. (2006) Androgen-
728 dependent pathology demonstrates myopathic contribution to the Kennedy disease phenotype
729 in a mouse knock-in model. *J. Clin. Invest.* 116:2663-2672. doi: 10.1172/JCI28773
- 730 Zuloaga, D. G., Morris, J. A., Jordan, C. L., & Breedlove, S. M. (2008) Mice with the testicular feminization
731 mutation demonstrate a role for androgen receptors in the regulation of anxiety-related
732 behaviors and the hypothalamic-pituitary-adrenal axis. *Horm. Behav.* 54:758-766. doi:
733 10.1016/j.yhbeh.2008.08.004

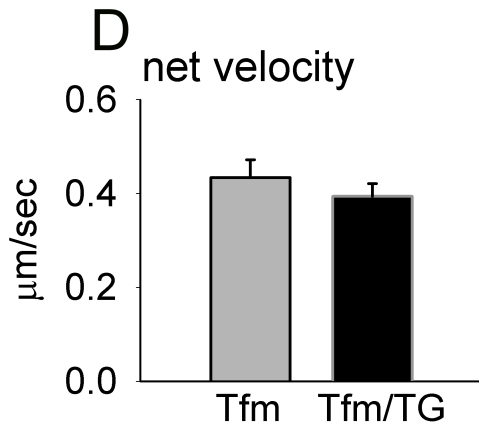
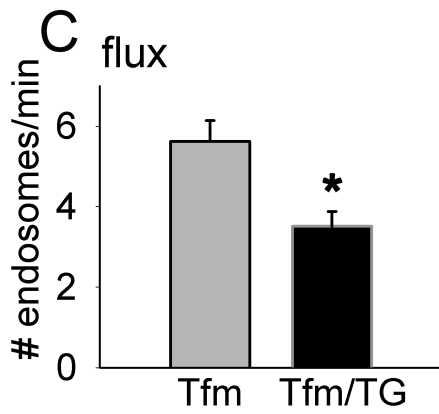
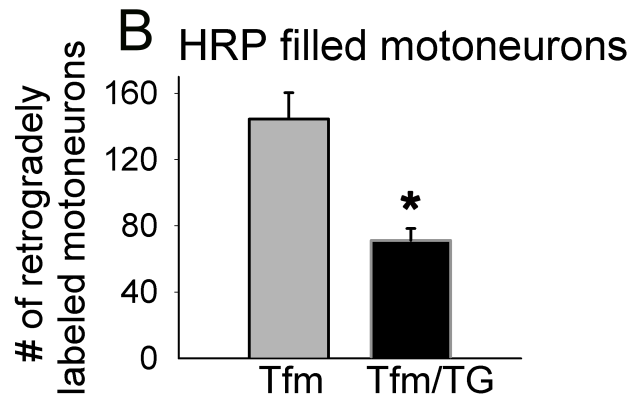
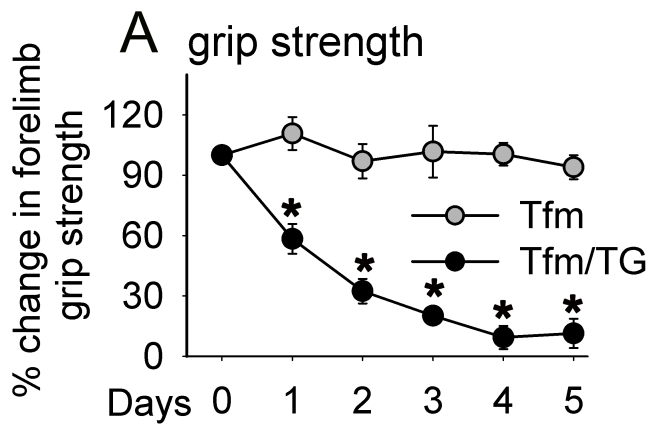
734

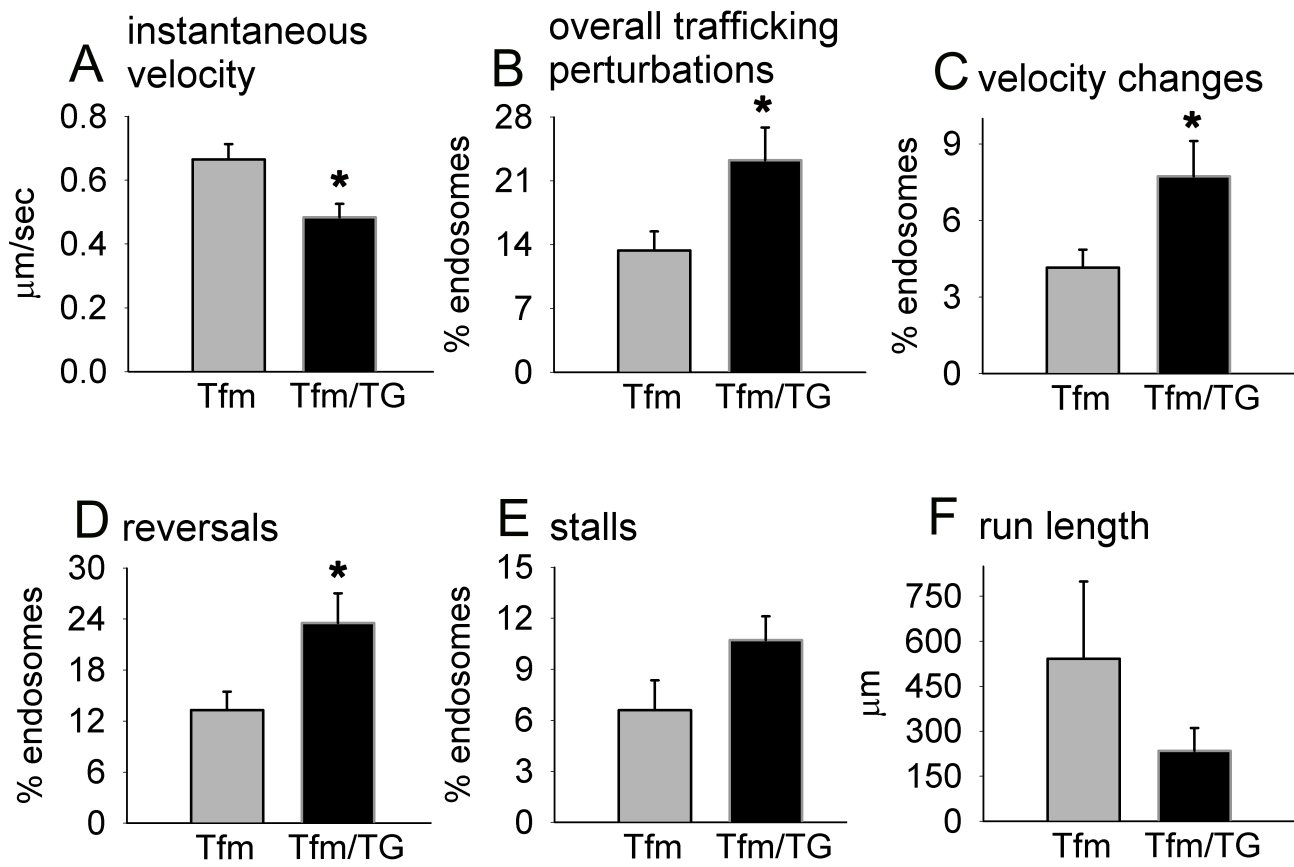


1 = stall

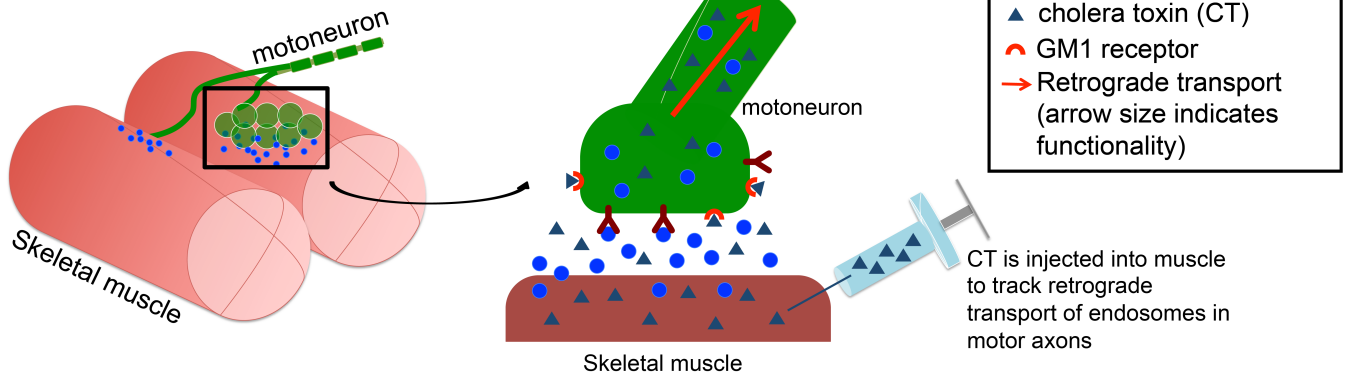
2, 3 = velocity change

4 = reversal





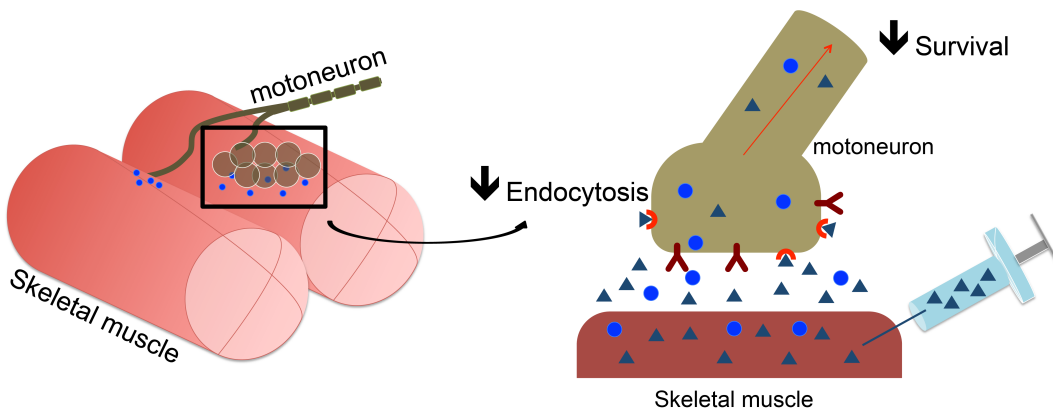
Healthy neuromuscular system (Tfm)



1. Normal production and release of NTFs from skeletal muscle

2. Muscle-derived NTFs enhance the uptake and retrograde transport of needed cargo to motoneuronal cell bodies to maintain their health and survival

Unhealthy (SBMA) neuromuscular system (Tfm/TG)



1. Reduced expression and release of NTFs from skeletal muscle

2. Deficits in muscle-derived NTFs impairs endocytosis (local, early event) and trafficking machinery (later event via possibly effects on gene expression) leading to long term demise and eventual death of motoneurons